INTERNATIONAL SOCIETY FOR SOIL MECHANICS AND GEOTECHNICAL ENGINEERING

SIMSG   ISSMGE

XVII European Conference
ECSMGE 2019
Reykjavík
on Soil Mechanics
and Geotechnical Engineering

Investigation of hydraulic heave in excavations using the material point method

Etude du soulèvement hydraulique dans les excavations en utilisant la méthode des points matériels

F. Fatemizadeh
Institute of Geotechnical Engineering/University of Stuttgart, Stuttgart, Germany

C. Moormann
Institute of Geotechnical Engineering/University of Stuttgart, Stuttgart, Germany

D. Stolle
Department of Civil Engineering/McMaster University, Hamilton, Canada

ABSTRACT: Owing to the total head difference between the inside and outside of an excavation, seepage occurs into the excavation. In cases where the head difference is large, the seepage velocities and resulting seepage forces can cause the catastrophic phenomenon of hydraulic heave inside the excavation, as well as overall basal instability. To investigate this phenomenon, the Material Point Method (MPM) has been employed in this study. MPM is a numerical procedure that accommodates large deformations and displacements of a continuum avoiding shortcomings of the classical Lagrangian finite element method. An in-house program, capable of modelling a biphasic medium as well as pure water in one model in the context of MPM was developed. Numerical results are presented and are compared to analytical predictions and the results of experimental investigations to verify the applicability of the modelling procedure.

RÉSUMÉ: En raison de la différence de hauteur totale entre l'intérieur et l'extérieur des excavations, des infiltrations se produisent dans l'excavation. Dans les cas où la différence de hauteur devient importante, la vitesse d'infiltration et en suivant la force d'infiltration augmentent, ce qui peut entraîner le phénomène catastrophique de soulèvement hydraulique à l'intérieur du site d'excavation, ainsi qu'une instabilité générale. Afin d'étudier ce phénomène, la méthode des points matériels (MPM) est adoptée dans cette étude. MPM est une procédure numérique qui accepte les grandes déformations et les déplacements d'un continuum et évite les inconvénients de la méthode des éléments finis lagrangiens classique. Un programme développé en interne, capable de modéliser un continuum biphasique ainsi que de l'eau pure dans un modèle dans le contexte du MPM, est adopté. Les résultats numériques sont présentés et comparés à ceux des méthodes analytiques et des enquêtes expérimentales afin de vérifier l'applicabilité de la procédure de modélisation.

Keywords: material point method; hydraulic heave; porous media; two phase medium; large deformation

1 INTRODUCTION

For excavations below the groundwater level a dewatering strategy is normally adopted to lower the water level and keep the excavation site dry. This results in a head difference between that forces water into the excavation.

As the head difference increases, the seepage velocities and the corresponding seepage forces increase, which can destabilize the soil at excavation, as well as causing hydraulic heave (Figure 1).
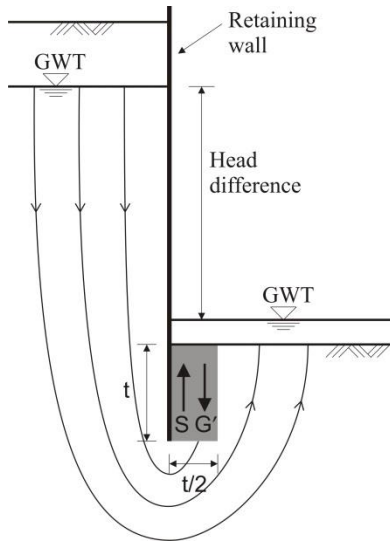

Figure 1. Hydraulic heave, Terzaghi's approach

This phenomenon is discussed in both the experimental and numerical literature. The experimental investigations go back to the work of Terzaghi at the beginning of twentieth century (Terzaghi 1925). There is considerable literature on this topic, including that of Koltuk (2017). His detailed experimental setup was capable of recording the pore water pressure in the sand along a retaining wall. He used Particle Image Velocimetry (PIV) to analyze the experimental data. Schober (2015) carried out detailed experimental investigations on hydraulic heave for excavations having a filter layer. He used the PIV method to identify the critical area near the retaining wall that is most likely to become unstable and provides detailed information about the failure process and the experimentally derived data. Alsaydalani and Clayton (2014) studied the fluidization of sand beds subject to vertical seepage forces.

Hydraulic heave has also been examined using numerical models. Aulbach (2013) adopted two and three dimensional Finite Element (FE) models for a detailed investigation of the phenomenon and showed that the rectangular area adjacent to the retaining wall which was assumed by Terzaghi as the region where hydraulic heave failure takes place is a good simplification for the prism-like failure mass which develops in experimental and numerical tests. Benmebarak et al. (2005) employed the commercial software FLAC 2D for their simulations. They varied the soil parameters and considered the corresponding effects on the hydraulic head loss. Fonte (2010) made use of the software package Plaxis for their finite element simulations of hydraulic heave in excavations. He studied the behaviour of both fine and coarse grained soils, and compared the shape of failure of each soil type. Numerical methods other than FEM have also been used; including, for example, Grabe and Stefanova (2015), who employed the smooth particle hydrodynamics method for their simulations, and Bolognin et al. (2017), who adopted the Material Point Method (MPM) for the simulation of fluidization in sand beds.

The classical Lagrangian FEM is capable of delivering results up to failure, but has difficulty to provide reliable information on the post failure behaviour of a liquefied soil. This is due to mesh tangling, which arises when dealing with large deformations. To avoid this problem, this study adopts the material point method (MPM) to simulate hydraulic heave. MPM is a numerical tool which is naturally capable of accomodating large deformations of continuum, avoiding the shortcommings of Lagrangian FEM. The material point method was developed for solid mechanics in 1990s by Sulsky et al. (1995), and Sulsky and Schreyer (1996). This method has been used to simulate different applications, including those in the field of geotechniques (Jassim 2013) and (Hamad 2014), to name a few. It has been adopted for the simulation of fully saturated soils; for example, by Jassim (2013) and Bandara (2013) who addressed problems dealing with saturated soils.

After a short review of the modelling framework and the governing equations for fully saturated soils in Section 2, a validation example, for which analytical solution exists, is presented in Section 3. It is used to validate the in-house programme developed for this study. In Section 4, the hydraulic heave phenomenon is simulated and the results are discussed. Finally, Section 5 presents some concluding remarks.

2 MATERIAL POINT METHOD

In MPM, a continuum is represented by material points (often referred to as particles), which act as "integration points" that move through a fixed background mesh. The working procedure of MPM in one time step (Figure 2) consists of mapping the data stored on material points to the nodes of mesh using standard shape functions (initialization phase). Thereafter the equations of motion are solved in the same manner as for classical FE method (solution phase). Finally the data are mapped back to the particles and the information are updated (convective phase).
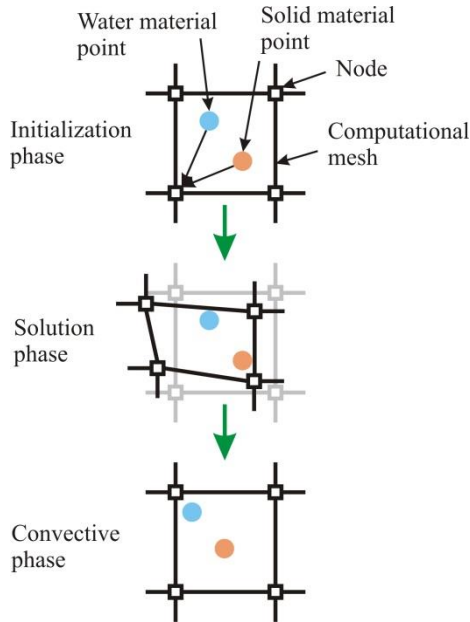

Figure 2. Working procedure of MPM

To represent a biphasic medium in the context of MPM two strategies are available. First, a single particle is used to define solid and water phases where a part of the material point represents the solid phase and the other part water phase. This method is adopted by Jassim (2013). The second strategy is to define each phase by separate particles. This method is adopted by Bandara (2013). In this study the second method is employed (Figure 3). By adopying this strategy free water (free surface water), pore water and solid grains can be simulated in one model which is necessary for the investigation of hydraulic heave.
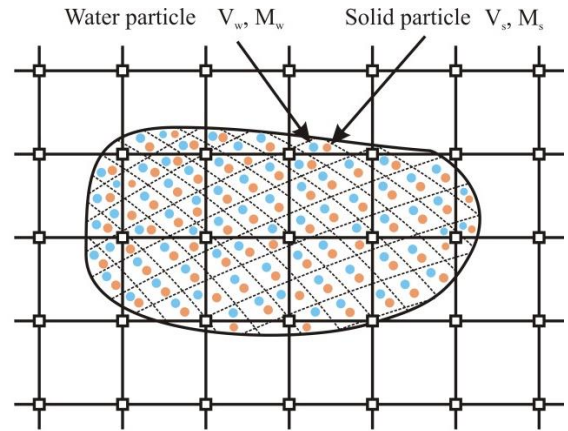

Figure 3. Discretization of MPM using two particle sets

The starting point in the two-phase dynamic MPM formulation is the momentum balance of the solid phase:

$$(1-n)\rho_s \boldsymbol{a}^s = \boldsymbol{\nabla} \cdot [\boldsymbol{\sigma}' + (1-n)\boldsymbol{\sigma}_w] + \frac{n^2 g \rho_w}{k} \cdot (\boldsymbol{v}^w - \boldsymbol{v}^s) + \boldsymbol{\sigma}_w \cdot \boldsymbol{\nabla} n + (1-n)\rho_s \boldsymbol{b} \quad (1)$$

where n is the porosity, ρ_s represents the solid grain density, $\boldsymbol{a}^s$ is the acceleration vector for the solid phase, $\boldsymbol{\sigma}'$ is the effective stress tensor and $\boldsymbol{\sigma}_w$ shows the water stress tensor for the free water, in which for the pore water it is replaced by pressure. The parameter g is the gravitational acceleration, ρ_w represents the water density

and $\boldsymbol{k}$ is the permeability tensor. Homogenous isotropic soil is considered here, for which the permeability is independent of direction, thus $\boldsymbol{k}$ can be replaced by k. The variables $\boldsymbol{v}^w$ and $\boldsymbol{v}^s$ are the water and solid velocity vectors, respectively, and $\boldsymbol{b}$ is the body force per unit mass. The momentum balance for the water phase can be written as:

$$\text{n}\rho_w \boldsymbol{a}^w = \boldsymbol{\nabla} \cdot (n\boldsymbol{\sigma}_w) - \frac{n^2 g \rho_w}{k} \cdot (\boldsymbol{v}^w - \boldsymbol{v}^s) + \boldsymbol{\sigma}_w \cdot \boldsymbol{\nabla} n + \text{n}\rho_w \boldsymbol{b} \tag{2}$$

where $\boldsymbol{a}^w$ is the acceleration vector for water. After deriving the weak form of the momentum balance equations and discretizing them in time and space, nodal accelerations for the solid and water phases can be calculated. Thereafter, particle velocities are obtained by integrating the nodal accelerations explicitly. Particle velocities are mapped to the nodes to determine the nodal velocities. In this stage, the mass balance equations of the solid and water are used to determine the water particle pressure keeping in mind that the solid grains are incompressible, with the water being slightly compressible and its density a function of pressure:

$$\frac{d}{dt}\text{p} = \frac{K_w}{n}[(1-n)\boldsymbol{\nabla} \cdot \boldsymbol{v}^s + n\boldsymbol{\nabla} \cdot \boldsymbol{v}^w] \tag{3}$$

in which p is the water pressure and K_w represents the bulk modulus of water. The nodal velocities are now integrated implicitly in time to get the nodal displacements. Thereafter the strains are updated, depending on particle positions and on the nodal displacements; i.e.,

$$\delta \boldsymbol{\varepsilon}^\alpha = \mathbf{B}\delta \boldsymbol{u}^\alpha \tag{4}$$

where $\boldsymbol{\varepsilon}^\alpha$ is the strain tensor with $\alpha = s, w$ phases, $\mathbf{B}$ is the strain-displacement matrix and $\delta \boldsymbol{u}^\alpha$ is the nodal displacement vector of the α phase during the current time step. At this stage the constitutive law of the solid phase is called to update the effective stress tensor and the constitutive law of the water phase is called to update the stress tensor of the free water particles. The nodal displacements are also used to update the position of each particle for the next time step.

At this stage, it must be checked that the volume occupied by the water particles in each element does not exceed the value allowed by the porosity of that element. For the case in which this condition is violated, the pressure of the water particles in that element are increased depending on the mass balance of the solid phase:

$$\Delta \text{p} = K_w \left(\frac{n_w}{n} - 1\right) \tag{5}$$

where Δp is the pressure correction due the violation of the water volume constraint and n_w is the actual porosity in the element. The parameter K_w is a large value. To eliminate drastic changes in pressure, a smaller value than K_w is adopted in equation (5) for this study.

3 VALIDATION EXAMPLE

Based on the formulation discussed in Section 2, an in-house program code was developed. To verify the validity of the program the Mandel-Cryer effect is simulated. In this problem a homogenous, isotropic and linear elastic fully saturated soil layer is confined between two rigid impermeable walls (Figure 4). A force is
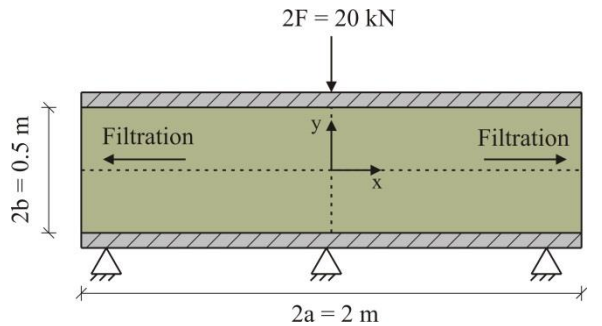
Figure 4. Geometry of the Mandel-Cryer example

suddenly applied on the walls and the excess pore water pressure generation at the middle of the soil layer is tracked. For this problem an analytical solution exists in the literature (Cheng and Detournay 1988).

The soil layer is assumed to have a permeability of $k = 10^{-5}$ $[m/s]$, porosity of $n = 0.4$, dry density of $\rho_d = 1680$ $[kg/m^3]$, Poisson's ratio of $\nu = 0.3$ and constrained elastic modulus of $E_c = 5$ $[GPa]$. Water has a bulk modulus of $K_w = 2$ $[GPa]$. The constrained elastic modulus of the soil is chosen to have the same stiffness in the soil and water so that the applied force is divided between water and soil equally at the beginning. Figure 5 shows the results obtained from the MPM simulation compared to the analytical solution for different dimensionless times. In this figure the excess pore water pressure on the positive x-axis (in the middle of the soil layer) is shown. Good agreement between the MPM simulations and the analytical results can be recognized.
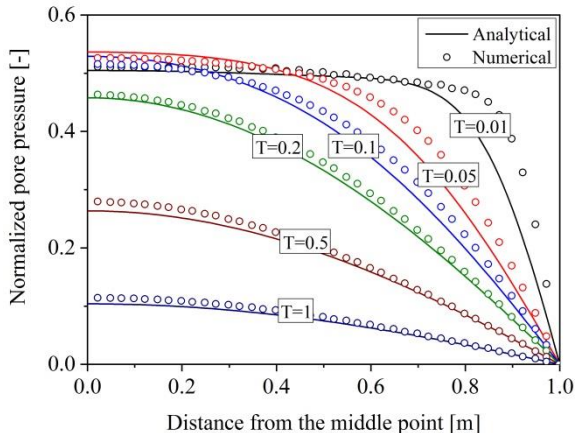

Figure 5. Results of the MPM simulation in comparison to analytical solution

4 HYDRAULIC HEAVE

A series of tests were conducted at the Institute of Geotechnical Engineering of the University of Stuttgart (Brandt 2015) to investigate the effect of construction errors for

retaining structures on the initiation of hydraulic heave. An MPM model is constructed to simulate one of the tests so the geometry is chosen to be as close as possible to that in the experiments. In this model (Figure 6) the sand with a height of 12 cm is placed over a 2 cm thick filter plate. Water is inserted into the sample at the bottom of the filter plate with a pipe that is attached to a water tank. The critical head difference in system at failure was recorded in experiment to be 23.05 cm. For the MPM model, the head difference given the mesh size is 24 cm.
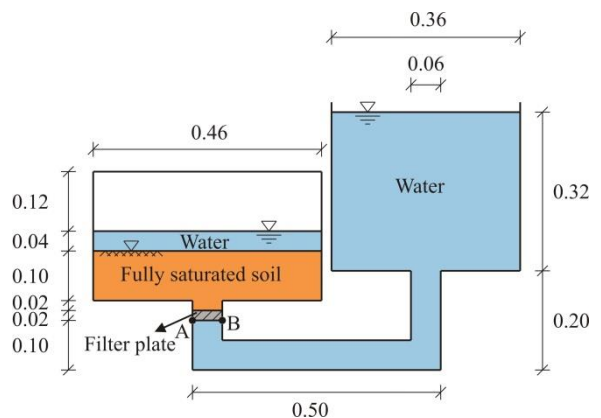

Figure 6. Schematic of the MPM model (all dimensions in meter)

The sand layer is modeled as elastic-perfectly plastic material following the Mohr-Coulomb failure criteria. Brandt (2015) provides some of the material parameters for the sand with the remaining values being assumed. The sand layer has a permeability of $k = 10^{-4}$ $[m/s]$, friction angle $\varphi = 30°$, dilation angle $\psi = 5°$, cohesion $c = 0$ $[Pa]$, grain density $\rho_s = 2650$ $[kg/m^3]$ and porosity $n = 0.4$. The Poisson's ratio $\nu = 0.3$ and elastic modulus $E = 10$ $[MPa]$. The filter plate is modeled as linear elastic material with permeability $k = 10^{-2}$ $[m/s]$, porosity $n = 0.4$, density $\rho_s = 2650$ $[kg/m^3]$, Poisson's ratio $\nu = 0.3$ and elastic modulus $E = 10$ $[MPa]$. Water is assumed to have a bulk modulus $K_w = 20$ $[MPa]$ and viscosity $\mu =$

10^{-3} [Pa·s]. The bulk modulus of water is reduced to increase the critical time step size needed for the dynamic simulations.

At first the valve in position AB (Figure 6) is closed so that the system reaches hydrostatic equilibrium. Thereafter the valve is opened and the water is allowed to flow through the filter plate into the system. In the MPM model the water pipe and the water tank are simulated to supply the head difference in the system as well as the water particles, which are needed to penetrate into the sand sample.

Figure 7 shows the displacement of the solid points at different time stages after the opening of the valve. In this figure, the water particles are turned off to focus on the behaviour of sand, but it should be kept in mind that the sand is always fully saturated during the simulation.

As can be seen in Figure 7, at the beginning the solid particles on the surface of the sand layer are fluidized due to the pressure waves applied from below on the sand and they start to swim in water. The particles on the surface are most affected by fluidization as there is no overburden pressure applied on them. The water particles coming from the water tank flows through the filter plate and push the sand layer upward. A small hole is produced above the filter plate (figure 7 top). As time proceeds the produced hole becomes bigger and more solid particles from the sand surface become fluidized and swim in water. As discussed before the hole is filled with water and the water level increases as well above the sand. Finally the water particles push the sand layer completely upward and the phenomenon of hydraulic heave is completed. The prediction from the numerical simulation is in good agreement with the observations from the experiments shown in the literature, especially those of Brandt (2015) and Alsaydalani and Clayton (2014) where they observe the same failure procedure. Figure 8 shows two pictures at two different time stages from the experiments of Brandt (2015) where the hole above the filter plate as well as failure state of the sand layer can be observed.
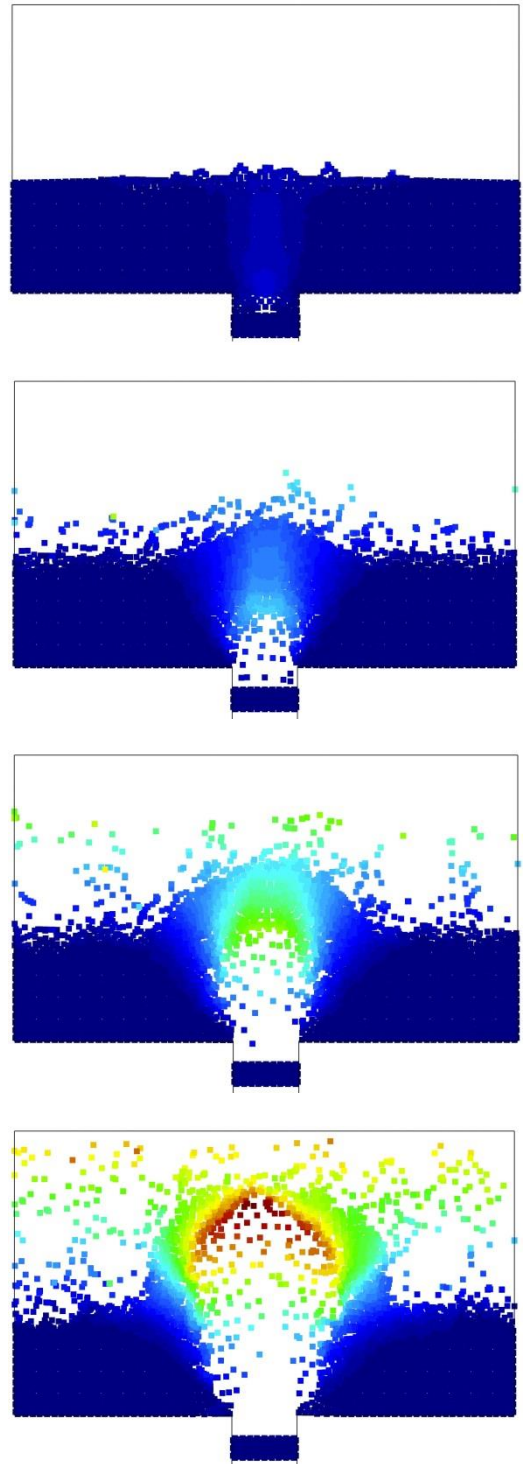

Figure 7. Displacement of soil grains at different time stages (dark blue zero with dark red 0.216[m])
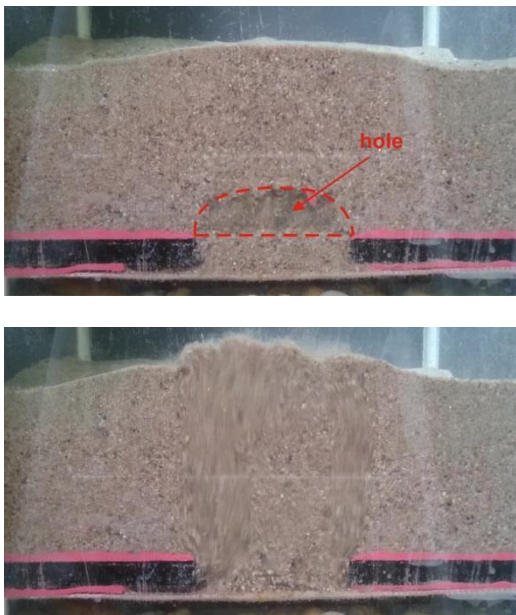
Figure 8. Experimental investigations of hydraulic heave (Brandt 2015)

5   CONCLUSIONS

After a short discussion regarding hydraulic heave and reviewing some previous numerical and experimental studies, the MPM was selected to investigate this phenomenon in more detail. The material point method was presented and an in-house developed program-code was validated by simulating the Mandel-Cryer effect and comparing the results with an analytical solution.

Finally, an experiment completed at the Institute of Geotechnical Engineering of the University of Stuttgart to investigate hydraulic heave was simulated using the MPM program. The stages predicted by the hydraulic heave simulation were also in good agreement with the experiment. In the numerical model almost the same head difference is adopted as in the experiment reported to be the critical value which initiated the failure.

There are still some points in the model, which can be improved in future; e.g., the material model and material parameters can be investigated in more detail and the mesh dependancy can be studied. The comparison between the experiments and simulation must also be done in more detail. All these points are currently being carried out by the authors.

6   REFERENCES

Alsaydalani, M.O.A., Clayton, C.R.I. 2014. Internal fluidization in granular soils, J*ournal of geotechnical and geoenvironmental engineering* **140**, 04013024-1–04013024-10.

Aulbach, B. 2013. *Hydraulic heave: the required embedded length for construction pits in non-cohesive soil*, RWTH Aachen University, Chair of Geotechnical Engineering, Aachen, Germany.

Bandara, S. 2013. *Material point method to simulate large deformation problems in fluid-saturated granular medium*, University of Cambridge, Geotechnical and Environmental Research Group, Cambridge, England.

Benmebarek, N. Benmebarek, S., Kastner, R. 2005. Numerical studies of seepage failure of sand within a cofferdam, *Computers and Geotechnics* **32**, 264–273.

Bolognin, M., Martinelli, M., Bakker, K.J., Jonkman, S.N. 2017. Validation of material point method for solid fluidisation analysis. *Procedia Engineering: Proceedings, 1st international conference on the material point method* (Eds: Rohe, A., Soga, K., Teunissen, H. & Coelho, B.Z.), 233-241. Elsevier Ltd., Amsterdam, Netherlands.

Brandt, R. 2015. *Simulation von hydraulischen Versagenszuständen bei Imperfektionen in wasserdichten Baugrubenkonstruktionen*, University of Stuttgart, Institute of Geotechnical Engineering, Master thesis, Stuttgart, Germany.

Cheng, A.H.D., Detournay, E. 1988. A direct boundary element method for plane strain poroelasticity, *International Journal for Numerical and Analytical Methods in Geomechanics* **12**, 551–572.

Fonte, J.B. 2010. *Numerical modeling of excavations below the water table*, Universidade Do Porto, Geotechnics Division, Master thesis, Porto, Portugal.

Grabe, J., Stefanova, B. 2015. Numerical modeling of saturated soils based on smoothed particle hydrodynamics (SPH) Part 2: Coupled analysis, Geotechnik **38**, 218–229.

Hamad, F. 2014. *Formulation of a dynamic material point method and applications to soil-water-geotextile systems*, University of Stuttgart, Institute of Geotechnical Engineering, Stuttgart, Germany.

Jassim, I. 2013. *Formulation of a dynamic material point method for geomechanical problems*, University of Stuttgart, Stuttgart, Germany.

Koltuk, S. 2017. *Investigations on the seepage failure by heave in excavation pits in non-cohesive soils*, RWTH Aachen University, Chair of Geotechnical Engineering, Aachen, Germany.

Schober, P. 2015. *Zum hydraulischen Grundbruch an Baugrubenumschließungen bei luftseitiger Sicherung durch einen Auflastfilter in nichtbindigen Böden*, Bundeswehr University Munich, Institute of Soil Mechanics and Foundation Engineering, Munich, Germany.

Sulsky, D., Schreyer, H.L. 1996. Axisymmetric form of the material point method with applications to upsetting and tylor impact problems, J*ournal Computer Methods in Applied Mechanics and Engineering* **139**, 409–429.

Sulsky, D. Zhou, S.J., Schreyer, H.L. 1995. Application of a particle-in-cell method to solid mechanics, *Computer Physics Communications* **87**, 236–252.

Terzaghi, K. 1925. *Erdbaumechanik*, Deuticke, Wien, Austria.